Driver-centred Autonomous Vehicle Motion Control within A Blended Corridor

Chongfeng Wei*, Richard Romano, Foroogh Hajiseyedjavadi***, Natasha Merat****, Erwin Boer*****

*Institute of Transport Studies, University of Leeds, Leeds, LS2 9JT UK (Tel: +44(0)113 343 0941; e-mail: c.wei2@ leeds.ac.uk).
**Institute of Transport Studies, University of Leeds, Leeds, LS2 9JT UK (e-mail: r.romano@leeds.ac.uk).
***Institute of Transport Studies, University of Leeds, Leeds, LS2 9JT UK (e-mail: f.hajiseyedjavadi@leeds.ac.uk).
****Institute of Transport Studies, University of Leeds, Leeds, LS2 9JT UK (e-mail: n.merat@its.leeds.ac.uk).
*****Institute of Transport Studies, University of Leeds, Leeds, LS2 9JT UK (e-mail: erwinboer@entropycontrol.com).

Abstract: As a potential cornerstone of the future intelligent transport system, autonomous vehicles (AVs) attract much attention of researchers across a wide range of areas from engineering to computer science. In addition, human factors issues, with respect to transfer of control and the interaction between the AVs and other road users have been studied. Current AV control algorithm development has focused on improving the safety of the vehicle, while the comfort of the drivers are normally ignored. Therefore, motion planning must not only avoid collisions between the vehicle and other road users and the road edges, but also needs to provide a sense of security and comfort for the drivers. Moreover, strict lane following can lead to overly cautious AVs relative to other road users, and thereby lead to traffic accidents. To solve these problems, we estimated the acceptable tolerance of the lateral offset based on the measured driving performance of real drivers and their reaction to a range of risk elements. Together with the vehicle dynamic constraints, the risk-based constraints are incorporated into a nonlinear Model Predictive Control (MPC) controller using a blended corridor. The result is a vehicle trajectory that produces a smooth motion within the corridor that considers the drivers' comfort.

Keywords: Model Predictive Control, Blended Corridor, Risk Elements, Driver-Centred

1. INTRODUCTION

As autonomous vehicles (AVs) are moving closer to reality, one of the key problems which still needs to be addressed is how to enable the vehicle to have a human-like driving performance. Pure collision avoidance and trajectory following cannot meet the requirements of future AVs as the sense of security and comfort are normally ignored, which may lead to the delay of the delivery of AV technologies.

Traditional path planning and following methods are widely developed and adopted for AV road tests (Paden et al., 2016). Normally, the path planning focuses on collision avoidance and lane keeping with the path following ensuring that the AV does not deviate too much from the planned path.

Different from robotics studies, the path planning work for the AVs need to involve the dynamic restrictions of the vehicles due to the limitations of tyre/road interaction, the stability of the vehicle and the mechanical manoeuvring action tolerances of the vehicle. Particularly, the tyre/road interaction limitations change dynamically with the road conditions. However, the path planning work rarely considers the sense of security and comfort for the drivers since most of the path planning contributions are just focusing on the safety issue. To provide a sense of security and comfort for the drivers, it is needed to incorporate the driver's expectations in the motion planning loop.

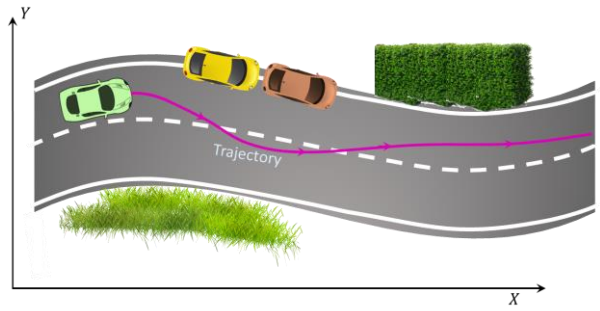

Fig. 1. Drivers' trajectory choice based on the surrounding risk elements on the road side

Path following research has been widely conducted to allow the vehicle to follow the planned path and correct the vehicle's manoeuvring behaviour even when the vehicle has a slight difference with the planned path (Hu et al. (2018a); (Macek et al., 2008). Too much focus on the corrections of the vehicle states overlooks the human drivers' personality and social intelligence (Li et al., 2018). Google is also working on reducing the accident probability due to the cautiousness of its autonomous car (Gu et al., 2017). The trajectory should not

simply avoid collisions but also guarantee the comfort for drivers around risk elements since parked vehicles, hedges, the road edge and even grass may bring a sense of wariness, as shown in Fig.1. Therefore, it is necessary to identify the passenger/driver's acceptable tolerance and range of security and comfort in terms of lateral offset tolerance and speed.

Another important factor is the vehicle dynamic boundaries resulting from the vehicle's own properties and the tyre/road interaction. These parameters determine the manoeuvrability of the vehicle within a given scenario. With the development of automated vehicles, some studies are starting to consider the vehicle's dynamic properties in the motion planning process. Recent planning approaches can be classified into four categories: graph search based plan (Karaman and Frazzoli, 2011; Soh Chin et al., 2011), sampling based plan (Hu et al., 2018b; Hwangbo et al., 2007), interpolating curve plan (Wang et al., 2018; Wei et al., 2017) and numerical optimization approach (Wei and Olatunbosun, 2014). To consider the vehicle constraints, speed and comfort elements, recent demonstrations have used optimal polynomial curves in terms of smoothness to deal with real implementations (Wei et al., 2017). However, due to the complex and fluctuating dynamic environment elements such as pedestrians, cyclists and other vehicles, the collision-free trajectory generation within the limited time is still an unsolved challenge.

Therefore when considering the sense of security and comfort for the drivers as well as the safety of the AVs, the path planning and path following approach can be replaced by another approach – corridor planning and motion control within the corridor. The corridor will be a blended corridor composed of the risk-led corridor and the vehicle dynamic corridor. The risk-led corridor is determined by the manoeuvre feedback (lateral offset, velocity and heading angle etc.) of the drivers to the risk elements (road hedge, hedge, grass, parked car and other moving vehicles), while the vehicle dynamic corridor is derived by the tyre/road interaction and the vehicle stability boundaries. Within the blended corridor, the AV control is able to provide a sense of security to the passengers/drivers and a smooth motion with a yaw rate and lateral acceleration that will guarantee the drivers comfort.

2. RISK-LED CORRIDOR MODEL

The focus of the risk model is to find acceptable vehicle states including lateral position and speed for specific roadway conditions. The navigation of the roadway by a human driver is an assessment of a range of acceptable vehicle states based on some criteria, which is defined as the level of perceived risk. It is assumed that the drivers perceive the current risk based on a maximum acceptable yaw rate error of the vehicle and a minimum time to lane crossing and accept lateral positions for which the vehicle will not depart the road given the minimum time and maximum yaw rate error (Boer, 2016).

The yaw rate error creates a cone of uncertainty around the heading of the vehicle at each point along the road. The cone of uncertainty is based on the driver's assumed perception and steering error (Boer, 2016). It projects the trajectory of the vehicle if continuing to travel with constant steering and speed. The assumption is that the driver controls the vehicle to keep the vehicle's *tlc* above an acceptable threshold. We refer to this threshold as minimum acceptable time to lane crossing (tlc_{min}). It is expected that tlc_{min} and acceptable yaw rate error varies across different roadway geometries, road furniture, and traffic conditions. This is explained by the driver attending more closely to the driving task in higher risk areas.

Based on a simple geometrical equation, the relationship between *tlc*, yaw rate error and vehicle's states is as follows (Boer, 2016).

$$V.tlc.\lambda = cos^{-1}\left(1 - \left(\frac{lw}{2} - \delta\right).\lambda\right) \quad (1)$$

Where V represents the vehicle's speed, *tlc* is time to lane crossing, λ is the yaw rate uncertainty, *lw* is the lane width and δ is the vehicle's offset from the centre of the lane.

A total number of 44 subjects between the age of 18 to 65 years (M=37.5, SD=12.8) participated in the driving simulation experiment at the University of Leeds Full Scale Motion Based Driving Simulator. All participants were required to have a valid UK driving license. The experiment was a complete within subject design and all the subjects have driven all the designed scenarios that involved 7 different independent factors including roadway environment including rural and urban, road curvature, curve radius, width of the road, roadside furniture, length of the presented roadside furniture, traffic condition.

The experimental design included 116 different scenarios (each representing one risk level) administered across 4 drives. Each scenario has been presented to the driver at least 4 times, 2 times with the presence of oncoming traffic and 2 times without any oncoming traffic. The order of the presented conditions was counterbalanced across subjects to account for the learning effect. Subjects has driven a practice drive before the actual session, and then two 40-45 minutes' sessions. All the subjects have been compensated for their time after finishing the experiments.

The observed speed and lateral position from the simulation experiment with the driving simulator is used to model the driving corridor. Fig. 2 shows the observed sets of speed and lateral position for a specific roadway condition (rural, wide, asphalt shoulder, curve to the right with oncoming traffic) as collected in the experiment. The horizontal axis shows the lateral position of the vehicle. The centre of the travel lane is define as 0 offset, negative values represent offset to the left side of the centre of the lane, and positive values represent offset toward the right side of the centre lane. Because of the multiple repetitions included in the experiment, observed lateral positions (the test data covered) are assumed to be acceptable while unobserved lateral positions (the test data did not cover) are considered unacceptable.

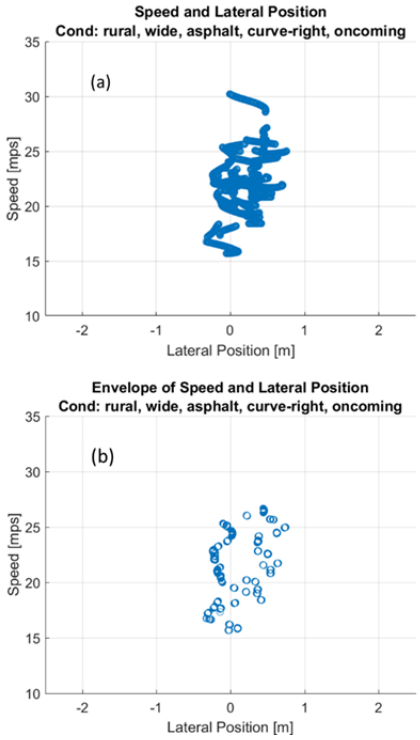

Fig. 2. (a) Observed Speed and Lateral Position from the Experiment at a Specific Road Condition, and (b) Boundary of the Data

In order to model the acceptable driving corridor the envelope of speed versus offset is extracted, Fig. 2 (b). To extract the envelope, the speed range is binned with 0.5 mps steps. The 95 percentile and 5 percentile of lateral offsets per speed bin represent right edge and left edge of the envelope, respectively. The idea of 95 percentile and 5 percentile is that those data points that are outside this range are already expected to be undesirable lateral position to most individuals.

As noted earlier, the cone of uncertainty when viewed as a lateral offset versus speed relationship follows an inverse cosine function (Eq. 1).

The final model is defined by 7 parameters. The maximum speed, the slope and intercept of the linear fit for the right and left edges and the maximum and minimum offsets in the constant segment. This set of 7 parameters per risk level gives the corresponding acceptable vehicle states.

Based on analysing the data from the driving simulator experiment, the left boundary and right boundary of the risk-led corridor for some different curve conditions at a speed of 10 m/s are shown in Table 1. It is noted that the Left and Right boundary data shown in Table 1 are relative to the centre of the lane, and the right direction is the positive lateral direction with regard to the centre of the lane.

Table 1. Risk-based corridor information

Curve direction	Context	Radius	Left boundary	Right boundary
'right'	'grass'	170 m	-0.57 m	0.76 m
'straight'	'asphalt'	9999 m	-0.46 m	0.56 m
'left'	'hedge'	250 m	-0.73 m	-0.27 m
'straight'	'blockage'	9999 m	1.18 m	2.12 m

A profile can be generated based on the risk corridor information by connecting sections of different curvatures together. An example risk-led corridor for a road profile composed of left and right curves and straight road is given in Fig. 3.(A). As the data has not been analysed to capture how the driver transitions between sections and so we have used a cosine curve transition between different sections with different boundaries. The processed corridor boundaries with transition is shown in Fig. 3.(B).

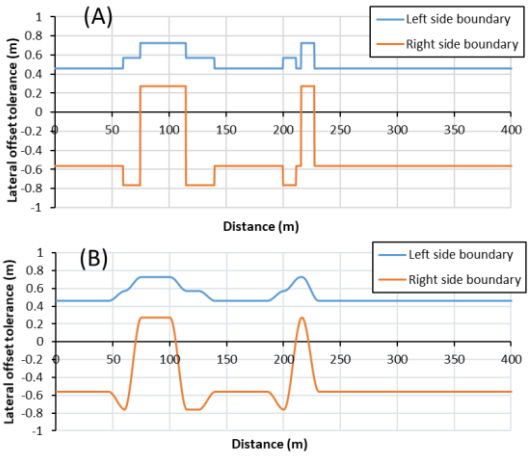

Fig. 3. Corridor generation for a hybrid road path with left and right curves and straight road: (A) without transition section, (B) with transition section

3. VEHICLE DYNAMIC MODEL

In this study, the vehicle dynamic model is simplified to a kinematic bicycle model, which is normally used for vehicle motion control as the suspension movement and rolling resistance influences are neglected. Fig. 4 shows the kinematic bicycle model in the global coordinate system and the deviation description relative to the road centre line path. We use the distance between the road centre line and the C.G. of the vehicle to define the deviation of the vehicle on the path.

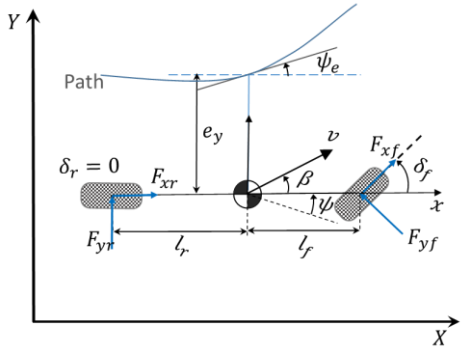

Fig. 4. Simplified kinematic bicycle model in the global coordinate system for vehicle dynamic control

In this case, the differential equations of the vehicle's motion in terms of lateral movement y, longitudinal movement x, yaw rate of the vehicle body $\dot{\psi}$, orthogonal distance e_y, the difference between the heading angle of the road and the heading angle of the vehicle e_ψ can be given as

$$\begin{cases} \ddot{y} = -\dot{x}\dot{\psi} + \frac{2}{m}\left(F_{yf}\cos\delta_f - F_{xf}\sin\delta_f + F_{yr}\right) \\ \ddot{x} = \dot{y}\dot{\psi} + \frac{2}{m}\left(F_{xf}\cos\delta_f - F_{yf}\sin\delta_f + F_{xr}\right) \\ \ddot{\psi} = \frac{2}{I_z}\left(l_f\left(F_{yf}\cos\delta_f + F_{xf}\sin\delta_f\right) - l_r F_{yr}\right) \\ X = \dot{x}\cos\psi - y\sin\psi \\ Y = \dot{x}\sin\psi + y\cos\psi \\ \dot{e}_y = \dot{y} + \dot{x}e_\psi \\ \dot{e}_\psi = \dot{\psi} - \frac{\dot{x}}{R} \end{cases} \quad (2)$$

where δ_f is the steer angle of the front wheel, R is the curve radius in real time, and it is equals to 9999 when the road is straight. I_z and m represent the vehicle's yaw inertia and mass, respectively. $\dot{x}$ and $\dot{y}$ denote the longitudinal and lateral speeds in the body frame and $\dot{\psi}$ denotes the yaw rate. F_{yf}, F_{xf}, F_{yr} and F_{xr} represent the lateral and longitudinal tyre forces at the front and rear wheels, in coordinate frames aligned with the wheels. The slip angle of the front and rear tyre are given as

$$\alpha_f = \tan^{-1}\left(\frac{\dot{y}+l_f\dot{\psi}}{\dot{x}}\right) - \delta_f \quad (3)$$

$$\alpha_r = \tan^{-1}\left(\frac{\dot{y}-l_f\dot{\psi}}{\dot{x}}\right) \quad (4)$$

For small tyre slip angles, the lateral tyre forces are normally defined as linearly proportional to the slip angle, which can be expressed as

$$F_{yf} = -c_f\alpha_f \quad (5)$$

$$F_{yr} = -c_f\alpha_r \quad (6)$$

4. MOTION CONTROLLER DESIGN

4.1 Discretization of the state space model

With the derived risk corridor and the vehicle dynamic model, the controller can be designed to control the motion of the vehicle system. Selecting global lateral position, longitudinal position, yaw angle, yaw rate, vehicle lateral deviation as output, then the continuous state space equation of the system can be expressed as

$$\dot{X}_s = A(t)X_s + B(t)u \quad (7)$$

$$Y_s = CX_s \quad (8)$$

where $X_s = [y, x, \psi, \dot{\psi}, Y, X, e_y, e_\psi]$, $Y_s = [y, \dot{\psi}, e_y, e_\psi]^{\mathrm{T}}$, $u = \delta_f$. If we express the nonlinear dynamic model of the vehicle system as $\dot{X}_s = f(X_s, u)$ then, $A(t) = \frac{\partial f}{\partial X_s}\Big|_{X_s(t),u(t)}$, $B(t) = \frac{\partial f}{\partial u}\Big|_{X_s(t),u(t)}$,

$$C = \begin{bmatrix} 1 & 0 & 0 & 0 & 0 & 0 & 0 & 0 \\ 0 & 0 & 0 & 1 & 0 & 0 & 0 & 0 \\ 0 & 0 & 0 & 0 & 0 & 0 & 1 & 0 \\ 0 & 0 & 0 & 0 & 0 & 0 & 0 & 1 \end{bmatrix}.$$

It is noted that only the front steering angle is considered as the input in this model, and the velocity of the vehicle kept constant. In this case, the longitudinal slip inputs can be ignored. The above state space equations of the vehicle system are continuous-time and cannot be used for the design of Model Predictive controllers directly. Thus, the model of the system is converted to a discrete state-space model by discretizing the state-space equations. If the Euler method is used to discretize the state-space model with an sample time of T_s , then the system can be described in discrete form

$$X_d(k+1) = A_d X_d(k) + B_d u(k) \quad (9)$$

$$Y_d(k) = C_d X_d(k) \quad (10)$$

where A_d, B_d and C_d are the discrete matrices for the state-space equation, respectively, which can be obtained by

$$A_d = e^{A(t)T_s}$$

$$B_d = \int_{kT_s}^{(k+1)T_s} e^{A(t)[(k+1)T_s-\tau]} B_d\, d\tau$$

$$C_d = C = \begin{bmatrix} 1 & 0 & 0 & 0 & 0 & 0 & 0 & 0 \\ 0 & 0 & 0 & 1 & 0 & 0 & 0 & 0 \\ 0 & 0 & 0 & 0 & 0 & 0 & 1 & 0 \\ 0 & 0 & 0 & 0 & 0 & 0 & 0 & 1 \end{bmatrix}.$$

4.2 Vehicle dynamic constraints

To guarantee the vehicle's safety and stability, the safety corridor should consider vehicle's dynamic performance and limit the vehicle's states into its dynamic corridor, and some important constraints need to be defined as follows.

I. Vehicle stability

To guarantee the stability of the vehicle, it is necessary to apply constraints to the side-slip angle of the vehicle and the yaw rate. The limitation of the slip-angle is different for road surfaces with different adhesion characteristics, and the constraint for the side-slip angle is to prevent the vehicle approaching the adhesion limitation. Similarly, it is also needed to constrain the yaw rate of the vehicle. Hence, the constraints of the side-slip angle and the yaw rate of the vehicle can be expressed as

$$\gamma_{\max} \le \gamma_{k+i,t} \le \gamma_{\min} \quad (11)$$

$$\beta_{\max} \le \beta_{k+i,t} \le \beta_{\min} \quad (12)$$

II. Vehicle's adhesion situation

Due to the tyre/road adhesion capability, the vehicle acceleration is bounded by the constant μg, where μ is the tyre/road friction coefficient and g is the gravitational acceleration. Thus, the vehicle's acceleration is subject to the following constraint:

$$\sqrt{a_x^2 + a_y^2} \le \mu g \quad (13)$$

In this study, constant speed is adopted, and thus the acceleration constraint can be reduced to

$$\left|a_y\right| \le \mu g \quad (14)$$

III. Vehicle's control and execution capability

As a mechanical system equipped with chassis active control systems, the vehicle's motion is limited by vehicle mechanical properties and electrical control system characteristics, which lead to the limits of the velocity control and the steering angle control. To make the vehicle's motion be smooth and safe, the vehicle's steering angle and their variations are constrained by

$$\delta_{f\min} \le \delta_{fk+i,t} \le \delta_{f\max} \quad (12)$$

$$\Delta\delta_{f\min} \le \Delta\delta_{fk+i,t} \le \Delta\delta_{f\max} \quad (13)$$

IV. Tyre's slip angle limitation

The tyre's slip angle cannot be obtained directly from the vehicle's dynamic output as it has not been defined as a vehicle state, but it can be calculated with linearization based on the vehicle's output values (see Eq.3 and Eq.4).

$$C_{\alpha i} = \frac{\partial \alpha_i}{\partial X_s} \qquad i = f, r \tag{15}$$

$$D_{\alpha i} = \frac{\partial \alpha_i}{\partial u} \qquad i = f, r \tag{16}$$

Therefore, the output of the slip angle can be expressed by the vehicle's states

$$\alpha_i = C_{\alpha i} X_s + D_{\alpha i} u \qquad i = f, r \tag{17}$$

To avoid the tyre's large slip at severe conditions, we use the following limitations of the front and the rear tyre's slip angle to make sure the relationship between the tyre lateral force and the slip angle is limited in the linear range

$$\alpha_{min} - \varepsilon \le \alpha_{f,k+i} \le \alpha_{max} + \varepsilon \tag{18}$$

With the above constraints, the stability of the closed loop system can be maintained. As the linear range of the relationship between lateral force and slip angle is maintained, the dynamic system is unable to enter into the possibly unstable region of the tyre characteristic.

4.3 Nonlinear MPC controller

Next, a Nonlinear MPC controller is designed to enable the on-board users to have a comfortable driving experience, and to improve the sense of security during cornering. One important property of MPC is receding horizon optimization, and the prediction of the vehicle's states and output variables is important to determine the control inputs within a specified horizon. The blended corridor derived from the risk corridor model and the vehicle dynamic limitations is used to define the constraints of the MPC, and the front wheel angle δ_f can be determined through the MPC controller and taken as an input for the vehicle dynamic system. To enable the vehicle to have a smooth motion within the blended corridor and to provide a sense of security and comfort for the drivers, we take zero yaw rate, road heading angle, zero lateral offset, and vehicle lateral velocity as the reference vehicle states, sufficient tolerances are given according to the drivers' intentions. The corresponding weighting factors are defined to mitigate the lateral vibration of the vehicle, and therefore, a comfortable driving experience within the corridor. The MPC problem can be synthesized as follows:

$$\min_{\Delta U(t)} \quad J(\xi_t, \Delta U(t)) = \sum_{i=1}^{N_p} \left\| Y_{k+i,t} - Y_{k+i,t}^{ref} \right\|_Q^2 + \sum_{i=1}^{N_c-1} \left\| \Delta u_{k+i,t} \right\|_R^2 + \rho \varepsilon^2 \tag{19}$$

$$s.t. \;\; X_d(k+i+1) = A_d X_d(k+i) + B_d u(k+i),$$
$$i = 0,1,\dots,N_p - 1$$
$$Y_d(k+i+1) = C_d X_d(k+i), \qquad i = 0,1,\dots,N_p - 1$$
$$u_{min} \le u_{k+i,t} \le u_{max}, \qquad i = 0,1,\dots,N_c - 1$$
$$\Delta u_{min} \le \Delta u_{k+i,t} \le \Delta u_{max}, \qquad i = 0,1,\dots,N_c - 1$$
$$Y_{min} - \varepsilon \le Y_d(k+i+1) \le Y_{max} + \varepsilon, \quad i = 1,2\dots,N_p$$
$$Yr_{min} \le Yr(k+i+1) \le Yr_{max}, \quad i = 1,2\dots,N_p$$

Where the constraint $Y_{min} - \varepsilon \le Y_d(k+i+1) \le Y_{max} + \varepsilon$ represents the limits of vehicle's states and other outputs that can be expressed by the vehicle's states, which include the vehicle's limits of lateral position, lateral acceleration, longitudinal speed, yaw rate, side slip angle and the tyres' slip angle. $Yr_{min} \le Yr(k+i+1) \le Yr_{max}$ denotes the risk corridor obtained from the human driving tests, as shown shown in Fig. 5.(B). The limitations of the steering angle and the increment of the steering angle are determined according to the vehicle's capabilities. In this study, the weighting factors and the controller parameters are defined as

$$Q = \begin{bmatrix} W_4 & 0 & 0 & 0 \\ 0 & W_3 & 0 & 0 \\ 0 & 0 & W_2 & 0 \\ 0 & 0 & 0 & W_1 \end{bmatrix}, N_p = 30, N_c = 5, R = 5\times10^3, \rho = 1000,$$

$$-10^o \le \delta_f \le 10^o, \; -0.85^o \le \Delta\delta_f \le 0.85^o, \; T = 0.05s, \mu = 0.8,$$

where

$$\begin{cases} W_1 = 2000, W_2 = 0, W_3 = 40, W_4 = 3000 & e_\psi > 0.1m \\ W_1 = 3000, W_2 = 10, W_3 = 40, W_4 = 3000 & |e_y - boundary| \le 0.3m \\ W_1 = 1000, W_2 = 0, W_3 = 20, W_4 = 3000 & 0.3 < |e_y - boundary| < 0.5m \\ W_1 = 0, W_2 = 0, W_3 = 20, W_4 = 3000 & else \end{cases}$$

and the boundary here represents the lateral offset boundary.

5. RESULTS AND DISCUSSION

The complex double-lane road profile given in Fig. 3 is used to evaluated the performance of the MPC controller. The results are shown in Fig. 5. The vehicle runs on the left side of the road according to the UK traffic rules. The risk corridor is derived based on driving simulator data. It can be seen that the derived corridor does not always include the lane centre line. The vehicle motion controller provides a smooth trajectory for the passengers/drivers within the risk corridor. In particular, in section 1, the vehicle has gentler cornering than the road path (lane centre line) curve, which aligns with the drivers' intention. In section 2, rather than following the road path, the vehicle has a tardier cornering behaviour with the proposed controller. That's because the road path is relatively sharp and emergency cornering may lead to the drivers being uncomfortable. Section 3 also shows a smoother motion behaviour of the vehicle compared to the road path. This smooth motion behaviour is more acceptable for the drivers as it provides more sense of security and comfort during cornering.

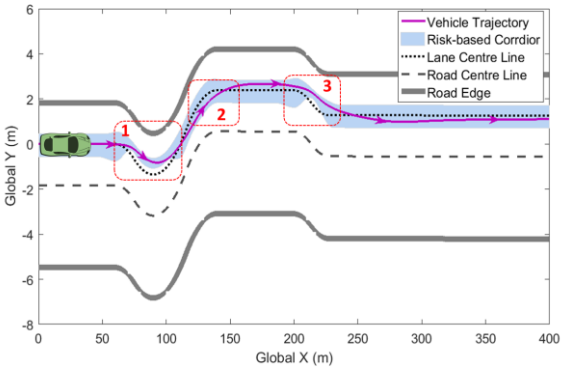

Fig. 5. Simulated vehicle trajectory with the blended corridor of a complex scenario

6. CONCLUSION

A risk corridor has been derived based on driving simulator tests with multiple drivers and risks. Together with the vehicle dynamic limitations, the risk corridor is used as a constraint for the vehicle motion control. A nonlinear MPC controller has been developed to provide the vehicle with a smooth motion within the blended corridor. The simulation results show that the Nonlinear MPC controller with a blended corridor will create a vehicle path that aligns with the drivers' intentions and provide a sense of security and comfort.

ACKNOWLEDGMENT

The work described in this abstract was undertaken in connection with the HumanDrive project which is co-funded by Innovate UK, the UK's innovation agency. This abstract is submitted with kind permission from the HumanDrive consortium: Nissan, Hitachi, Horiba MIRA, Atkins Ltd, Aimsun Ltd, SBD Automotive, University of Leeds, Highways England, Cranfield University and the Connected Places Catapult.

REFERENCES

Boer, E.R., 2016. Satisficing Curve Negotiation: Explaining Drivers' Situated Lateral Position Variability. *IFAC-PapersOnLine* 49(19), 183-188.

Gu, Y., Hashimoto, Y., Hsu, L.-T., Iryo-Asano, M., Kamijo, S., 2017. Human-like motion planning model for driving in signalized intersections. *IATSS Research* 41(3), 129-139.

Hu, C., Qin, Y., Cao, H., Song, X., Jiang, K., Rath, J.J., Wei, C., 2018a. Lane keeping of autonomous vehicles based on differential steering with adaptive multivariable super-twisting control. *Mechanical Systems and Signal Processing*.

Hu, C., Wang, R., Yan, F., Huang, Y., Wang, H., Wei, C., 2018b. Differential Steering Based Yaw Stabilization Using ISMC for Independently Actuated Electric Vehicles. *IEEE Transactions on Intelligent Transportation Systems* 19(2), 627-638.

Hwangbo, M., Kuffner, J., Kanade, T., 2007. Efficient Two-phase 3D Motion Planning for Small Fixed-wing UAVs, *Proceedings 2007 IEEE International Conference on Robotics and Automation*, pp. 1035-1041.

Karaman, S., Frazzoli, E., 2011. Sampling-based algorithms for optimal motion planning. *The International Journal of Robotics Research* 30(7), 846-894.

Li, L., Ota, K., Dong, M., 2018. Humanlike Driving: Empirical Decision-Making System for Autonomous Vehicles. *IEEE Transactions on Vehicular Technology* 67(8), 6814-6823.

Macek, K., Philippsen, R., Siegwart, R., 2008. Path following for autonomous vehicle navigation with inherent safety and dynamics margin, *2008 IEEE Intelligent Vehicles Symposium*, pp. 108-113.

Paden B., Čáp M., Yong S. Z., Yershov D. and Frazzoli E., 2016, A Survey of Motion Planning and Control Techniques for Self-Driving Urban Vehicles, in *IEEE Transactions on Intelligent Vehicles*, 1(1), pp. 33-55,

Soh Chin, Y., Parasuraman, S., Ganapathy, V., 2011. Dynamic path planning algorithm in mobile robot navigation, 2011 IEEE Symposium on Industrial Electronics and Applications, pp. 364-369.

Wang, Y., Zhou, Z., Wei, C., Liu, Y., Yin, C., 2018. Host-Target Vehicle Model-based Lateral State Estimation for Preceding Target Vehicles Considering Measurement Delay. IEEE Transactions on Industrial Informatics, 1-1.

Wei, C., Olatunbosun, O.A., 2014. Transient dynamic behaviour of finite element tire traversing obstacles with different heights. Journal of Terramechanics 56, 1-16.

Wei, C., Olatunbosun, O.A., Yang, X., 2017. A finite-element-based approach to characterising FTire model for extended range of operation conditions. Vehicle System Dynamics 55(3), 295-312.